

The Crystal Structure of Human Eukaryotic Release Factor eRF1—Mechanism of Stop Codon Recognition and Peptidyl-tRNA Hydrolysis

Haiwei Song,*† Pierre Mugnier,‡
Amit K. Das,† Helen M. Webb,‡
David R. Evans,§ Mick F. Tuite,‡
Brian A. Hemmings,§ and David Barford*†||

*Section of Structural Biology
Institute of Cancer Research
237 Fulham Road
London, SW3 6JB
United Kingdom

†Laboratory of Molecular Biophysics
University of Oxford
Oxford, OX1 3QU
United Kingdom

‡Department of Biosciences
University of Kent
Canterbury, CT2 7NJ
United Kingdom

§Friedrich Miescher-Institut
Maulbeerstrasse 66
CH-4058 Basel
Switzerland

Summary

The release factor eRF1 terminates protein biosynthesis by recognizing stop codons at the A site of the ribosome and stimulating peptidyl-tRNA bond hydrolysis at the peptidyl transferase center. The crystal structure of human eRF1 to 2.8 Å resolution, combined with mutagenesis analyses of the universal GGQ motif, reveals the molecular mechanism of release factor activity. The overall shape and dimensions of eRF1 resemble a tRNA molecule with domains 1, 2, and 3 of eRF1 corresponding to the anticodon loop, aminoacyl acceptor stem, and T stem of a tRNA molecule, respectively. The position of the essential GGQ motif at an exposed tip of domain 2 suggests that the Gln residue coordinates a water molecule to mediate the hydrolytic activity at the peptidyl transferase center. A conserved groove on domain 1, 80 Å from the GGQ motif, is proposed to form the codon recognition site.

Introduction

Termination of protein biosynthesis and release of the nascent polypeptide chain is signaled by the presence of an in-frame stop codon at the aminoacyl (A) site of the ribosome. The process of translation termination is universal and is mediated by protein release factors and GTP (reviewed by Buckingham et al., 1997; Nakamura and Ito, 1998). A class 1 release factor recognizes the stop codon and promotes the hydrolysis of the ester bond linking the polypeptide chain with the peptidyl (P) site tRNA, a reaction catalyzed at the peptidyl transferase center of the ribosome. Class 2 release factors,

which are not codon specific and do not recognize codons, stimulate class 1 release factor activity and confer GTP dependency upon the process (Milman et al., 1969; Grentzmann et al., 1994; Mikuni et al., 1994; Stansfield et al., 1995a; Zhouravleva et al., 1995). Release factors were characterized initially in prokaryotes, where two similar proteins, RF1 and RF2, function as class 1 release factors, whereas a structurally unrelated protein, RF3, was identified as the class 2 release factor (Scolnick et al., 1968). Both class 1 release factors recognize UAA; however, UAG and UGA are decoded specifically by RF1 and RF2, respectively. Eukaryotic protein biosynthesis occurring on cytosolic ribosomes is terminated by the release factors eRF1 and eRF3 (Frolova et al., 1994; Stansfield et al., 1995a; Zhouravleva et al., 1995). Although eRF1 is the functional counterpart of prokaryotic RF1 and RF2, the protein is unrelated in primary structure to the prokaryotic proteins and functions as an omnipotent release factor, decoding all three stop codons (Goldstein et al., 1970; Konecki et al., 1977; Frolova et al., 1994). Class 2 factors (RF3 and eRF3) are GTP-binding proteins (Grentzmann et al., 1994; Zhouravleva et al., 1995). RF3 is active as a GTPase on the ribosome in the absence of RF1/2 (Freistroffer et al., 1997), whereas the eRF3 GTPase activity requires the additional presence of eRF1 (Frolova et al., 1996), possibly because eRF1 and eRF3 form functional complexes (Stansfield et al., 1995a; Zhouravleva et al., 1995). Overexpression studies in mammalian cells and in vitro reconstitution assays have indicated that eRF1 alone is sufficient to promote efficient termination, implying that eRF3 is nonessential for the termination reaction in these organisms (Frolova et al., 1994), although yeast viability is dependent on eRF3 (Stansfield et al., 1995a).

The molecular mechanisms by which release factors decode stop codons and promote ribosome-catalyzed peptidyl-tRNA hydrolysis remain obscure. Functionally, class 1 release factors mimic tRNA molecules. For example, a number of studies indicate direct interactions between the stop codon and class 1 release factors. First, early studies from Tate and colleagues demonstrated that prokaryotic RF1 and RF2 are capable of being chemically cross-linked to stop codons encoded within minimessenger RNA molecules when associated with the ribosome (Tate et al., 1990; Brown and Tate, 1994). Extension of these studies suggested that RF2 also interacts with as many as three bases immediately 3' to the stop codon (Poole et al., 1997). This is consistent with the discovery of base bias 3' to the stop codon in both prokaryotes and eukaryotes (Brown et al., 1990; Poole et al., 1995) and that in yeast and *Escherichia coli* the bases flanking the stop codon influence the efficiency of termination (Bonetti et al., 1995; Poole et al., 1995; Mottagui-Tabar et al., 1998). Second, release factors catalyze the release of fMet from ribosome-fMet-tRNA^{fMet}-stop codon complexes, in a release factor-specific manner. For example, RF1 will catalyze the release of fMet from ribosomes loaded with fMet-tRNA^{fMet} in the presence of UAA or UAG but not UGA, whereas RF2 catalyzes release in the presence of UAA or UGA

|| To whom correspondence should be addressed (e-mail: dbarford@icr.ac.uk).

but not UAG. More recent data utilizing mini-mRNA templates have indicated that release factors recognize the stop codon in frame with a sense codon at the P site (Grentzmann and Kelly, 1997; McCaughan et al., 1998). There is also evidence that the binding sites of tRNAs and release factors overlap at the A site of the ribosome, since the activity of release factors is competitive with that of suppressor tRNA molecules (Eggertsson and Soll, 1988).

The notion that release factors structurally mimic tRNA molecules has been advanced to explain their functional mimicry (Moffat and Tate, 1994; Ito et al., 1996), prompted by the finding that the structure of the elongation factor EF-G (Ævarsson et al., 1994; Czerwowski et al., 1994) resembles the tRNA-EF-Tu complex (Nissen et al., 1995). On the basis of a proposed sequence relationship between class 1 release factors and domains III-V of EF-G, which are reminiscent of the anticodon loop and T stem of a tRNA molecule, Nakamura and colleagues (Ito et al., 1996) suggested that class 1 release factors are structural mimics of tRNA molecules. Recently, sequence analysis of class 1 release factors revealed the existence of a GGQ sequence motif that is universal to all species and critical for release factor activity (Frolova et al., 1999). Substitutions of the motif-Gly residues abolished the ability of human eRF1 to trigger peptidyl-tRNA hydrolysis, suggesting that this motif stimulates the hydrolytic activity of the peptidyl transferase center (Frolova et al., 1999).

To provide insights into the molecular mechanisms by which eRF1 promotes hydrolysis of the peptidyl-tRNA bond, decodes stop codons, and interacts with eRF3 and PP2A, and to address the question of tRNA mimicry, we determined the crystal structure of human eRF1 to 2.8 Å resolution and performed a functional analysis of the role of the GGQ motif in yeast eRF1 (Sup45p). The structure reveals a likely role for the conserved GGQ motif at the peptidyl transferase center of the ribosome and indicates the binding sites for eRF3 and PP2A. By correlating sequence conservation data and the position of yeast eRF1 mutants that enhance ribosomal stop codon readthrough, we have mapped the codon recognition region onto the molecule.

Results and Discussion

Structure Determination

The crystal structure of human eRF1 was determined using a combination of MIRAS and MAD procedures, yielding an interpretable electron density map at 3.1 Å that allowed the placement of over 80% of the protein sequence, a process aided by seven selenomethionine sites (Table 1). Refinement of the partial model using CNS (Brünger et al., 1998) and the calculation of electron density maps from combined phases and later $2F_o - F_c$ maps allowed the remainder of the ordered regions of the structure to be determined. The final structure includes residues 5 to 422. Three regions of the polypeptide are not visible in the electron density map and are assumed to be disordered, namely residues 333–342 and 358–370 and 15 residues at the C terminus. The working and free R factors obtained using data between 30 and 2.8 Å are 0.246 and 0.314, respectively (Table 1).

Overall Architecture

The polypeptide chain of eRF1 is organized into three domains of similar size with a structure reminiscent of the letter Y (Figure 1). Domain 2 is positioned on the stem of the Y and participates in few interdomain contacts with domain 3 and none with domain 1. All three domains belong to the twisted α - β sandwich architectural class, each with a mixed β sheet core surrounded on both sides by α helices. The topologies of the three domains differ from one another and represent unique folds. Domain 1 is composed of a four-stranded β sheet surrounded on both sides by two α helices. Helices α -2 and α -3 form an anti parallel helix hairpin that packs against one face of the β sheet to form a prominent groove at the helix- β sheet interface, a structural feature that may play a role in codon recognition. The N terminus of the protein is formed by the α -1 helix of domain 1, which also creates the interface with domain 3. The connection to domain 2 is made by an extended region of chain linking α -4 of domain 1 with the central β strand of the β sheet of domain 2. The architecture of domain 2 is characterized by the excursion of the N terminus of the α -5 helix by 25 Å away from the main body of the domain. At the N terminus of this helix, and most remote from the remainder of the molecule, the chain forms a tight turn formed from residues of the conserved sequence motif $^{181}\text{GRGGQS}^{186}$ (Figure 2). This motif is connected to the edge β strand of domain 2 by an extended segment of chain lacking secondary structure. Domains 2 and 3 are bridged by a long α helix, kinked at the domain interface. Domain 3 deviates slightly from a standard α - β sandwich fold by the insertion between the α -10 helix and central β sheet of a disordered segment of chain (residues 334 to 369). Although a portion of this region forms a small structured β sheet, the majority of the residues are either poorly ordered or not visible in the electron density map.

Comparison with Bacterial and Mitochondrial Class 1 Release Factors

On average, the pair-wise sequence identity of eukaryotic and Archaea class 1 release factors is 30%, suggesting that the release factors from these two kingdoms will share similar structures (Figure 2). In contrast, no significant similarity exists between the eukaryotic and Archaea RFs sequences and their prokaryotic and mitochondrial counterparts, suggesting the existence of two distinct protein families (Frolova et al., 1994). Moreover, we expect that these two families will adopt different protein architectures since a secondary structure prediction based on 34 multiply aligned prokaryotic RF1/RF2 and mitochondrial RF sequences indicated a pattern of α helices and β strands that would be inconsistent with the 3-domain α - β organization of eRF1.

Although the two families of release factors appear to be unrelated, a striking feature of all release factors is the occurrence of a universal GGQ sequence motif (Figure 2) (Frolova et al., 1999). Moreover, in all known sequences, the GGQ motif occurs within a context rich in arginine and lysine residues, suggesting a universal and essential function in release factor activities.

Table 1. Crystallographic Data Statistics for Human eRF1

	Data Set			
	Native	HgCl ₂	TMLA	TMLA + HgCl ₂
Data Collection and MIR Phasing Statistics				
X-ray source (SRS)	PX9.6	PX7.2	PX9.6	PX9.6
Wavelength (Å)	0.87	1.47	0.87	0.87
Resolution (Å)	2.7	3.2	3.0	3.5
Observations (N)	82,505	56,394	121,827	35,528
Unique reflections (N)	16,712	10,088	12,011	9,602
Completeness (%)	99.2 (98.0)	99.3 (97.2)	99.4 (100)	94.3 (98.0)
Anomalous completeness (%)	—	95.5 (92.1)	99.5 (100)	84.6 (90.7)
Multiplicity	4.9 (3.5)	5.6 (3.5)	10.1 (6.7)	3.7 (3.7)
R _{merge} ^a (%)	5.0 (40.6)	5.7 (59.9)	6.6 (49.9)	5.8 (44.3)
R _{anom} (%)	—	4.9 (46.6)	3.5 (17.8)	7.7 (29.3)
I/σ	8.3 (1.9)	7.0 (1.2)	5.8 (1.5)	4.7 (1.7)
MIR Phasing Statistics				
R _{deri} ^b (%)		34.2	27.5	39.3
Heavy-atom sites (N)		3	1	4
Phasing power ^d acentric/centric		1.46/0.93	1.07/0.69	1.53/1.00
R _{cullis} ^c acentric/centric		0.76/0.81	0.89/0.89	0.78/0.81
Figure of merit ^f	0.75			
MAD Data Collection and Phasing Statistics (EMBL, BW7A)				
	Data Set			
	λ1	λ2	λ3	λ4
Wavelength (Å)	0.9790	0.9793	0.9350	0.9789
Resolution (Å)	3.2	3.2	3.2	3.2
R _{merge} ^a (%)	5.4 (31.1)	5.4 (27.8)	4.7 (25.5)	5.3 (24.4)
R _{anom} (%)	6.6 (22.3)	5.3 (18.5)	5.4 (18.1)	7.0 (20.5)
Completeness (%)	99.9 (99.7)	99.9 (99.7)	99.8 (99.7)	99.8 (99.7)
Anomalous completeness (%)	99.9 (99.7)	99.8 (99.7)	99.8 (99.6)	99.5 (97.2)
Observations (N)	52,201	51,409	49,891	44,725
Unique reflections (N)	13,458	13,455	13,451	13,444
Multiplicity	3.9 (4.0)	3.8 (3.9)	3.7 (3.8)	3.3 (3.2)
I/σ	8.2 (2.4)	8.2 (2.7)	9.1 (3.0)	8.0 (3.0)
MAD Phasing Statistics^e				
Phasing power ^d acentric/centric	3.41/3.00	2.89/2.22	—	2.77/2.16
Anomalous phasing power	1.62	1.05	1.40	1.72
R _{cullis} ^c acentric/centric	0.59/0.56	0.50/0.46	—	0.53/0.49
Anomalous R _{cullis}	0.82	0.94	0.88	0.79
Figure of merit ^f	0.81			
Refinement Summary				
Resolution range (Å)		20.0–2.8		
Reflections (N)		14,553		
Protein atoms (N)		3,228		
Water molecules (N)		110		
R value ^g		24.6		
Free R value ^h		31.4		
Deviation from idealityⁱ				
Bond lengths (Å)		0.014		
Bond angles (°)		2.0		

Values in parentheses are for the highest resolution shell.

^a R_{merge} = $\sum_n \sum_j | \langle I(h) \rangle - I(h) | / \sum_n \sum_j \langle I(h) \rangle$, where $\langle I(h) \rangle$ is the mean intensity of symmetry-equivalent reflections.

^b R_{deri} = $\sum ||F_{PH}| - |F_p|| / \sum |F_p|$, where |F_{PH}| and |F_p| are the structure-factor amplitudes of the derivative and native data, respectively.

^c R_{cullis} = $\sum | (F_{PH} - F_p) - F_H | / \sum |F_{PH} - F_p|$.

^d Phasing power = F_H/E_{RMS}, where F_p, F_H and F_{PH} are the structure factors for the native, heavy atoms, and derivative, respectively, and E_{RMS} is the residual lack of closure.

^e MAD phasing was calculated as a special case of MIRAS, where λ3 was used as native, and other wavelength data were used as individual derivatives.

^f Figure of merit after density modification.

^g R value = $\sum ||F_{obs}| - |F_{calc}|| / \sum |F_{obs}|$, where F_{obs} and F_{calc} are the observed and calculated structure factors, respectively.

^h The free R value was calculated using 6% of the data. Root-mean-square deviations relate to the Engh and Huber parameters.

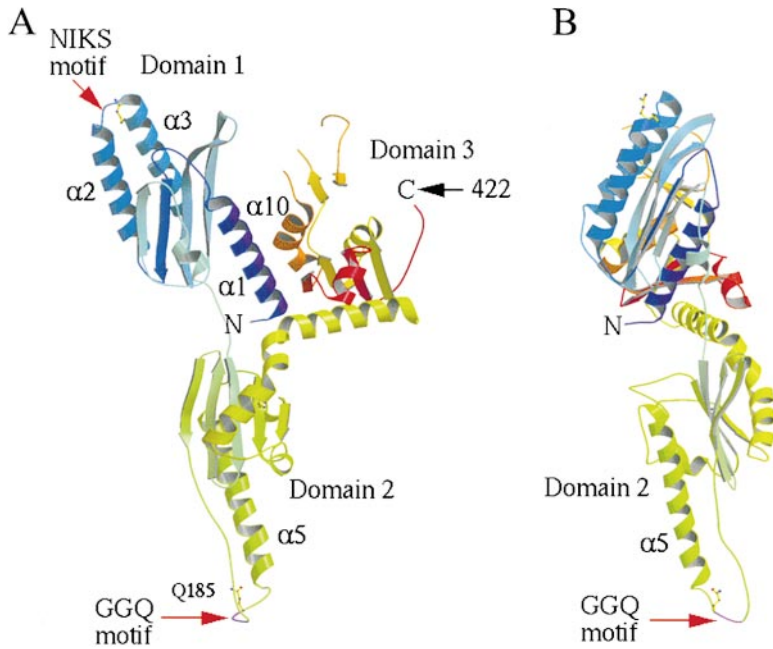


Figure 1. Orthogonal Views of eRF1
The figure indicates the position of the GGQ sequence motif at the tip of domain 2 and the suppressor mutant Arg-68 on the α -2/ α -3 helix hairpin of domain 1. Figure produced by MOLSCRIPT (Kraulis, 1991) and RASTER3D (Merit and Murphy, 1994).

Role of the GGQ Motif in Translation Termination

To examine the role of the invariant Gln residue of the GGQ motif in release factor activity, we tested the ability of yeast eRF1 bearing substitutions of the GGQ motif residues to support viability or to lead to a termination-deficient phenotype. Site-directed mutagenesis was

used to replace Gln-182 (Gln-185 in human eRF1) with Leu, Arg, or Pro. In addition, Gly-180 or Gly-181 (equivalent to Gly-183 and Gly-184 of human eRF1) was replaced with Ala, Val, or Asp to generate both single or double mutants. The termination defect was tested by *SUC5* tRNA^{Ser}-mediated stop codon readthrough of the

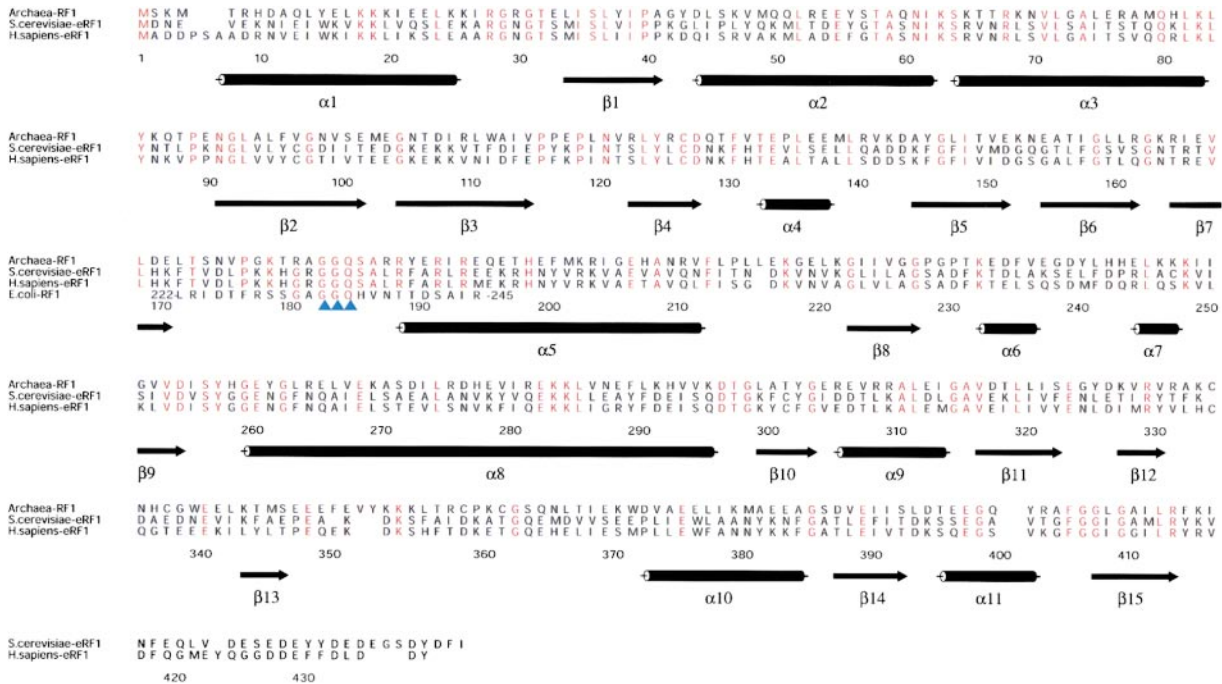


Figure 2. Multiple Sequence Alignment of Class 1 Release Factors

Human eRF1, *S. cerevisiae* eRF1 (*SUP45*), and Archaea (*Pyrococcus abyssi*) RF1 were aligned using MULTALIGN (Barton, 1990). Invariant residues are colored red. The GGQ motif is denoted with blue arrows, and the corresponding *E. coli* RF1 sequence is aligned below. Secondary structure elements are indicated. Figure drawn using ALSCRIPT (Barton, 1993).

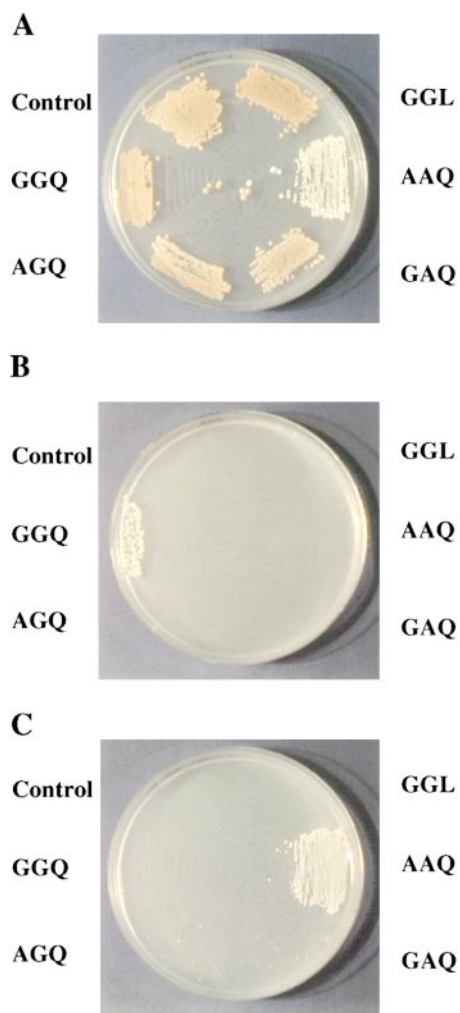


Figure 3. Amino Acid Changes in the GGQ Motif Lead to Nonfunctional eRF1 In Vivo in Yeast

Haploid strain Δ LE2[pUKC803] in which the chromosomal *sup45::HIS3* disruption is complemented by a *URA3* plasmid encoding *SUP45* was transformed with mutated derivatives of pUKC1901 and subsequently grown on either YEPD media (A) or Minimal Medium containing 5FOA (B and C). The plasmid, pRS315, which lacks *SUP45*, was used as the control.

(A) Four derivatives of this plasmid were tested that encode modified eRF1 where GGQ has been modified as AGQ, GAQ, AAQ, or GGL, respectively. None of the mutants tested were dominant lethal at 30°C. The double mutant G180A-G181A generated an Ade⁺ white phenotype.

(B) After loss of the *URA3* plasmid, none of the mutants could support viability when compared to the wild-type-eRF1. Identical results were obtained for the Q182R and Q182L mutants (data not shown). (C) The G180A, G181A, and G180A-G181A double mutants display dominant-negative phenotypes, conferring adenine prototrophy on the strain.

ochre *ade2-1* allele leading to adenine prototrophy, while viability was tested after elimination of the *URA3* plasmid carrying wild-type eRF1. All the mutants grew on selective or rich medium at 30°C prior to the elimination of the wild-type eRF1 gene indicating that none of them had a dominant-lethal effect over the wild-type protein (Figure 3A). Elimination of the *URA3* plasmid, carrying the wild-type copy of eRF1, in cells producing

eRF1 modified at any position 180, 181, or 182 was lethal since no viable FOA transformants were obtained on 5-fluoroorotic acid (FOA) selection (Figure 3B). Only substitutions of the GGQ motif residues caused lethality, since mutations elsewhere in the GGQ minidomain (for example S179R) had an identical phenotype to the wild-type protein (P. M., H. M. W., and M. F. T., unpublished data).

In addition to being nonfunctional, yeast eRF1 with mutations of the GGQ motif Gly residues exhibits a dominant-negative phenotype by permitting the weak ochre suppressing *SUQ5* tRNA^{Ser} to translate the *ade2-1* ochre allele gene containing an internal in-frame ochre stop codon. The double mutant G180A-G181A grew on Minimal Medium lacking adenine whereas wild-type could not, and those containing either the G180A or the G181A change displayed a slow growth (Figure 3C). These data indicate that the G180A-G181A mutant competes with the wild-type protein for the internal ochre codon of the *ade2-1* gene, although it does not lead to a loss of viability. Our results demonstrating that residues of the GGQ motif are critical for the in vivo function of eRF1 agree with a recent study using an in vitro assay that the ability of human eRF1 to trigger peptidyl-tRNA hydrolysis is abolished by alterations of the GGQ motif Gly residues (Frolova et al., 1999). Human eRF1 with single Gly substitutions is dominant-negative in vitro, inhibiting the peptidyl-release activity of wild-type eRF1. Moreover, mutation of the GGQ motif Gly residues does not impair the ability of eRF1, together with the ribosome, to induce eRF3 GTPase activity (Frolova et al., 1999). Our genetic data, together with the biochemical data of Frolova et al. (1999), indicate that all residues of the GGQ motif function to promote the hydrolytic activity of the peptidyl transferase center but that the GGQ motif is not involved in either codon recognition or ribosome and eRF3 interactions.

Structure of the GGQ Motif

Within the eRF1 structure, the GGQ motif is located on a turn connecting an extended region of β strand with the N terminus of the α -5 helix, a structural feature that forms the tip of the eRF1 molecule and creates a self-autonomous GGQ minidomain (Figures 1 and 4). This minidomain is stabilized by conserved hydrophobic interactions involving Leu-176 and Pro-177 of the strand and Phe-190 and Leu-193 of the α -5 helix. Pro-177 is invariant within all eukaryotic and Archaea RF1 sequences, and the reduced flexibility of the protein main-chain conferred by the proline may contribute to structural stabilization. The conformation of the Gln-185 residue of eRF1 is stabilized by a network of hydrogen bonds involving invariant residues of the GGQ minidomain. Its side-chain amide group accepts a hydrogen bond from the guanidinium group of the invariant Arg-189 residue and in turn, the main-chain amide group of Arg-189 donates a hydrogen bond to the hydroxyl-group of Ser-186. The GGQ minidomain is abundant in Arg and Lys residues, a feature that creates a marked positive electrostatic potential on the protein surface (Figure 4B).

Class 1 release factors function to coordinate a water molecule at the peptidyl transferase center of the ribosome at the same position as an amino group of an A site aminoacyl tRNA molecule. Nucleophilic attack of

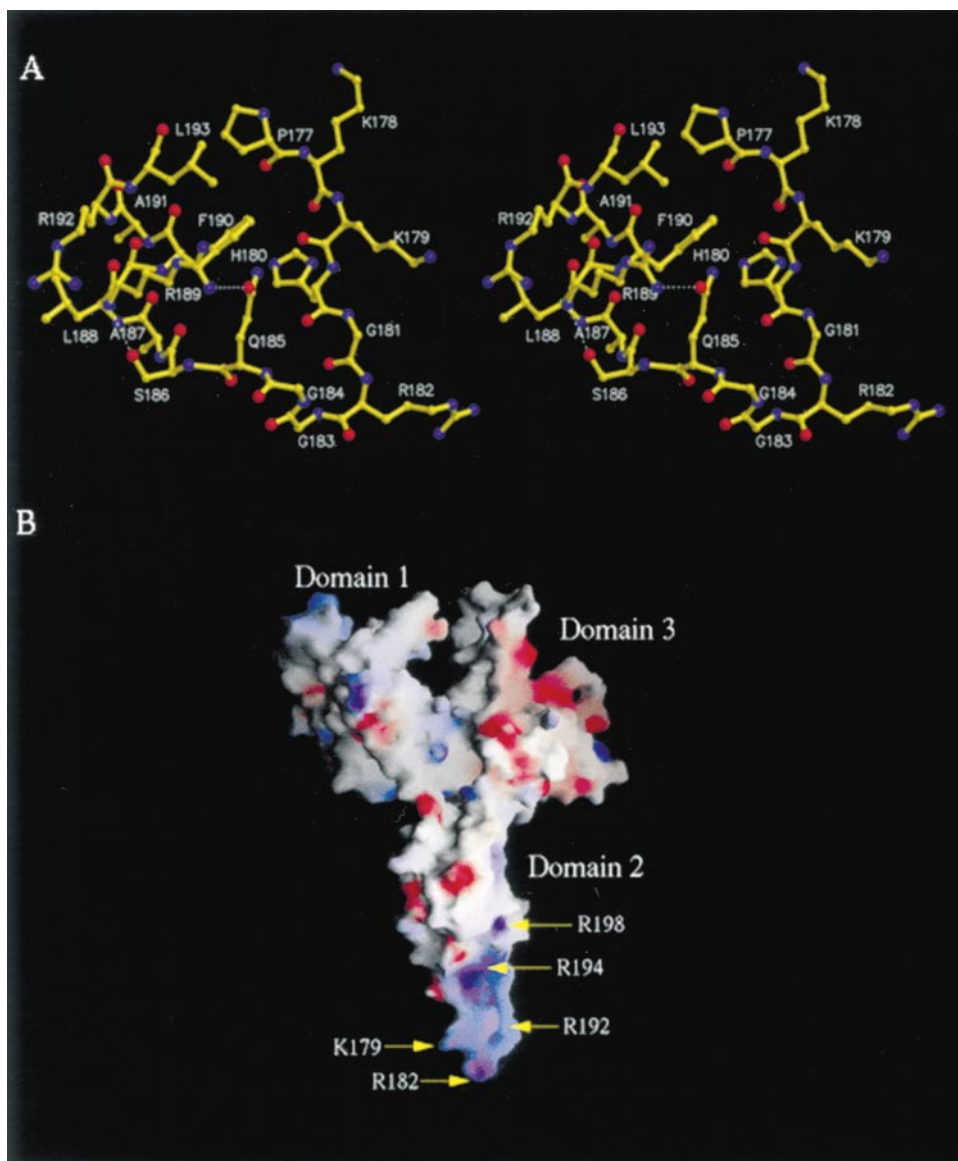


Figure 4. Detailed View of the GGQ Minidomain

(A) Stereo view of residues Pro-177 to Leu-193. The view is rotated 180° relative to Figure 1A.

(B) Solvent accessible surface and electrostatic potential of eRF1 viewed as in Figure 1A. The figure reveals the positive electrostatic potential of the GGQ minidomain. Arg and Lys residues of the GGQ minidomain are labeled. Figure produced using GRASP (Nicholls et al., 1991).

the ester bond of the peptidyl-tRNA molecule in the P site by a water molecule, promoted by a release factor at site A, releases the nascent polypeptide chain, whereas attack by the amino group of an aminoacyl tRNA molecule in site A elongates the polypeptide chain (Figure 5). Apart from the difference in the nature of the nucleophilic attacking group, these two reactions are essentially identical and may share the same catalytic machinery at the peptidyl transferase center. The position of the GGQ motif at the exposed tip of domain 2, its essential function and universal occurrence in all class 1 release factors, suggests that the GGQ residues of this motif play a direct role at the catalytic site of the peptidyl transferase center. We propose that Gln-185 of the GGQ motif participates in the coordination of the water molecule at the peptidyl transferase center responsible for hydrolyzing the peptidyl-tRNA ester bond (Figure 5B).

eRF3 and PP2A Interaction Sites Are Contained within Domain 3

Deletion mutagenesis studies combined with two-hybrid and direct binding analyses have provided semi-qualitative information concerning the eRF3 binding site on eRF1. Residues 281–415 of human eRF1 are necessary and sufficient for the interaction with eRF3 (Merkulova et al., 1999), a region that corresponds exactly to the core secondary structure of domain 3, demonstrating that an intact domain 3 is required for eRF1-eRF3 interactions. Crucially, loss of the highly conserved residues 411–415 abolishes eRF1 interactions with eRF3 (Merkulova et al., 1999). Residues 410–415 form β -15, one of the central β strands of the domain 3 β sheet, and deletion of these residues would be likely to destabilize the entire domain. The extreme C terminus of eRF1 (residues 416–437), which is rich in acidic residues, is

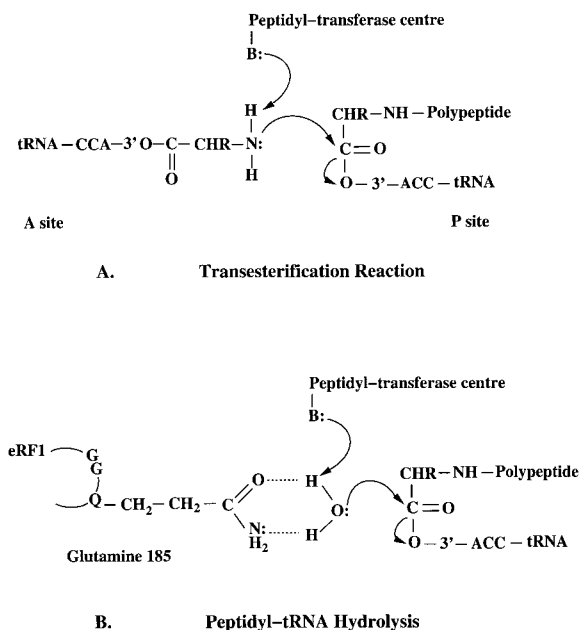


Figure 5. Schematic of the Reactions Catalyzed at Peptidyl Transferase Center of the Ribosome

(A) Transesterification reaction.

(B) Proposed scheme for hydrolysis of the peptidyl-tRNA bond in site P by a catalytic water molecule coordinated by Gln-185 of the eRF1 GGQ motif in site A.

required for high-affinity eRF1/eRF3 interactions in budding and fission yeast (Ito et al., 1998; Eurwilaichitr et al., 1999). However, studies with human eRF1 demonstrate that a form of the protein lacking the C-terminal 22 amino acids is active as a release factor, stimulating hydrolysis of fMet-tRNA^{fMet}. In addition, the protein is capable of interacting with eRF3 and stimulating eRF3 GTPase activity (Merkulova et al., 1999). Within the human eRF1 electron density map, these residues are disordered and are assumed to be mobile regions of the protein.

In addition to eRF3 interactions, domain 3 serves other functions. For example, in yeast, interactions with the ribosome require the entire C terminus of eRF1 (Eurwilaichitr et al., 1999), although ribosome interactions may be mediated via eRF3 whose association with eRF1 would have been diminished in these studies. In vertebrates, 1% of the protein serine/threonine phosphatase PP2A is associated with eRF1 (Andjelkovic et al., 1996), an interaction mediated by residues Thr-338 to Asn-381 of domain 3 of eRF1.

Stop Codon Decoding Site and tRNA Mimicry

The activities of class 1 release factors depend upon their ability to recognize and interact with stop codons and concomitantly trigger the hydrolytic activity at the peptidyl transferase center. Release factors functionally mimic tRNA molecules not only by recognizing mRNA codons within the small subunit but also by interacting at the peptidyl transferase center of the large subunit and by association with a GTPase. To explain these characteristics, and in the context of the structural similarity between EF-G and a tRNA-EF-Tu complex (Nissen et al., 1995) and the proposed sequence similarity between EF-G and *E. coli* RF1/RF2, the concept of tRNA

mimicry by class 1 release factors was proposed (Ito et al., 1996). Our structure of eRF1 provides an opportunity to assess these predictions. The overall shape and dimensions of eRF1 bear some resemblance to that of a tRNA molecule (Figure 6). The width of eRF1 of 71 Å matches the 70 Å of phenylalanine tRNA. However, although, eRF1 and tRNA have a similar thickness of 27 Å and ~22 Å, respectively, eRF1 is some 15 Å longer than tRNA. It is also possible that the conformation of eRF1 that we observe in the crystal differs from that bound to the ribosome and/or the one in complex with eRF3. Conformational flexibility of domain 2 relative to domains 1 and 3 would be facilitated by the relatively few interactions between domain 2 and the remainder of the molecule.

A comparison of the eRF1 and tRNA structures suggests that the functional similarities of these two molecules are reflected in structural equivalencies. For example, the GGQ motif of eRF1 is equivalent to the aminoacyl group attached to the CCA-3' sequence of the aminoacyl stem of a tRNA molecule. Both groups interact at the peptidyl transferase center of the ribosome with contrasting consequences (Figure 5). Consistent with equivalent functional roles, both groups are located on exposed, distal positions of their respective molecules, with the GGQ motif located on the tip of an extended β turn α helix minidomain and the tRNA aminoacyl group on the CCA-3' acceptor stem (Figures 6 and 7). The similar and characteristic positions of the GGQ motif and the aminoacyl group may allow equivalent interactions with the peptidyl transferase center, suggesting that domain 2 of eRF1 is the structural counterpart of the aminoacyl acceptor stem of tRNA. Another functional characteristic shared by eRF1 and tRNA is the association with the GTPases eRF3 and EF-Tu/eEF-1α, respectively. EF-Tu interacts with the tRNA T stem and aminoacyl acceptor stem, whereas eRF3 interacts with domain 3 of eRF1, suggesting a functional equivalence between domain 3 of eRF1 and the T stem of tRNA. Domain 3 of eRF1 is structurally equivalent to the T stem of a tRNA molecule (Figure 6).

Previously, no functional role had been ascribed to domain 1, although the structure of domain 1 is highly conserved from eukaryotes to the Archaea, and replacement of Arg-65 with a Cys residue in yeast eRF1 leads to an omnipotent suppressor phenotype (Mironova et al., 1986). Mapping the degree of conservation shared between eukaryotic eRF1 and Archaea RF sequences onto the molecular surface reveals a prominent region of structural conservation, corresponding to a shallow groove formed from the interface created by the antiparallel α-2 and α-3 helical hairpin and the central antiparallel β sheet of domain 1 (Figure 7). The role of eRF1 to interact both with stop codons and the peptidyl transferase center suggests that the distance between the codon and peptidyl-transferase interaction sites will match that between the anticodon bases and the amino group of the aminoacylated tRNA molecule, a distance of ~75 Å (Figure 7). Our proposal for the role of Gln-185 of the GGQ motif implies that its side chain is equivalent to the amino group of an aminoacyl-tRNA molecule. The site of structural conservation on domain 1 of eRF1 is situated ~80 Å from the side chain of Gln-185. This groove and the associated exposed face of the α-2 and

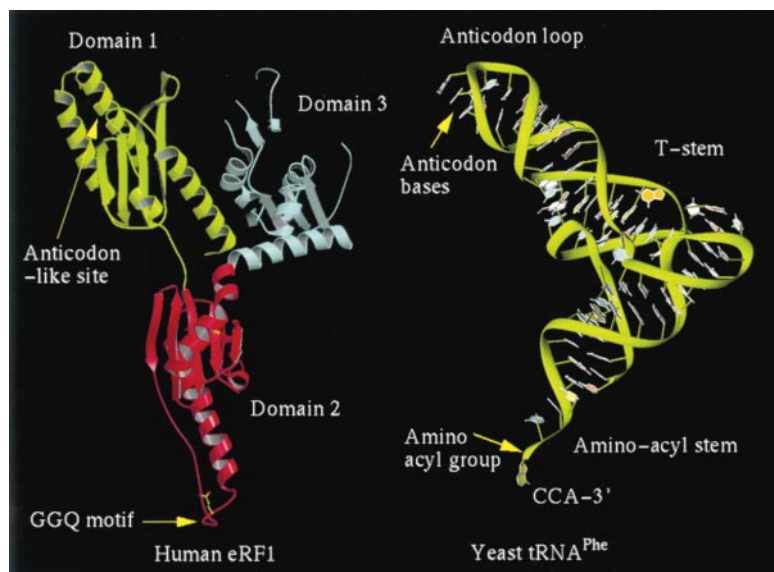


Figure 6. Molecular Mimicry of tRNA Molecules

Ribbon diagram of eRF1 and yeast tRNA^{Phe} structures, revealing similar shapes and overall dimensions. The disposition of domains 1, 2, and 3 of eRF1 matches those of the tRNA anticodon loop, aminoacyl stem, and T stem, respectively. The site of attachment of an aminoacyl group at the CCA stem is indicated.

α -3 helices is likely to represent the stop codon interaction site of eRF1, a notion suggested by its high structural conservation, the appropriate distance to the GGQ motif, and the overall size of the groove that matches the anticodon bases of a tRNA (Figure 7). The small discrepancy in distance between the GGQ motif and proposed anticodon site of domain 1, and the tRNA CCA stem and anticodon bases, may result from the requirement to accommodate a catalytic water molecule at the peptidyl transferase center. The model for codon recognition involving domain 1 that we present here is supported by a recent mutagenesis analysis of yeast eRF1 by Stansfield and colleagues. Their analysis identified novel omnipotent suppressor *sup45* mutants that are defective in the recognition of all three stop codons. However, these mutants exhibit increased ratios of UGA relative to UAG stop codon suppression when compared with those of the *sup45-2* temperature-sensitive allele, which has a general defect in ribosome binding (Stansfield et al., 1995b, 1997). This finding infers that the novel mutations produce specific UGA stop codon recognition defects. Strikingly, all mutations map to domain 1, with 7 out of 8 mutations situated on the α -2 and α -3 helices and β strands that line the proposed codon recognition groove (I. Stansfield and G. Bertram, personal communication).

The structure of the *Thermos thermophilus* ribosome in complex with tRNA at 7.8 Å resolution revealed that the tRNA bound to the A site forms relatively few contacts with the ribosome, except for the anticodon loop and aminoacyl stem (Cate et al., 1999). However, the A site tRNA molecule packed close to and in parallel with the P site tRNA molecule, bringing the amino acid at the 3' end of the A site aminoacyl tRNA molecule into close proximity with the peptidyl-tRNA bond of the P site peptidyl tRNA. A stop codon present at the A site directs an eRF1 molecule to interact with the P site peptidyl-tRNA in a manner analogous to that of an aminoacyl tRNA molecule. These functional requirements of eRF1 impose structural constraints upon the molecule, which may be satisfied by adopting a similar overall structure to a tRNA molecule.

Conclusion

The crystal structure of eRF1 presented here, combined with an analysis of regions of structural conservation throughout eukaryotes and the Archaea, coupled with yeast eRF1 mutagenesis data, provides a framework for understanding the molecular mechanisms of release factor activity. We propose that the GGQ motif triggers the hydrolytic activity of the peptidyl transferase center by facilitating the coordination of a water molecule that performs the nucleophilic attack onto the peptidyl-tRNA ester bond. The universal and essential nature of a glutamine argues in favor of a model whereby its amide side chain functions to coordinate the catalytic water molecule. Such a function for the Gln residue would be reminiscent of the Gln residues at the catalytic sites of GTPases (Scheffzek et al., 1997) and protein tyrosine phosphatases (Pannifer et al., 1998) that coordinate water molecules for GTP and cysteinyl-phosphate hydrolysis, respectively. The peptidyl transferase activity of prokaryotic ribosomes involves the 23S RNA molecule (Noller et al., 1992). Conserved Gly and basic residues of the GGQ minidomain may function to allow contacts with the phosphate backbone of either the peptidyl transferase center RNA and/or the CCA stem of the P site tRNA molecule. A conserved groove present on domain 1 is proposed to function as the codon recognition site. The position of the groove relative to the GGQ motif, the conservation of residues within the groove, and the mapping of stop codon suppressor mutations to this region, are all consistent with its role as the anticodon site of eRF1. The architecture of domain 1 bears no resemblance to the RNA recognition motif (RRM) characteristic of numerous RNA binding proteins (Nagai et al., 1995). However, structures of aminoacyl tRNA synthetases demonstrate that the tRNA anticodon binding motifs of diverse protein architectures are capable of mediating protein-RNA interactions. The proposed codon recognition groove of eRF1 features polar and hydrophobic residues, consistent with the observed nature of protein-RNA interactions.

Our structural data allows a reevaluation of the tRNA mimicry hypothesis. The structure of eRF1 displays

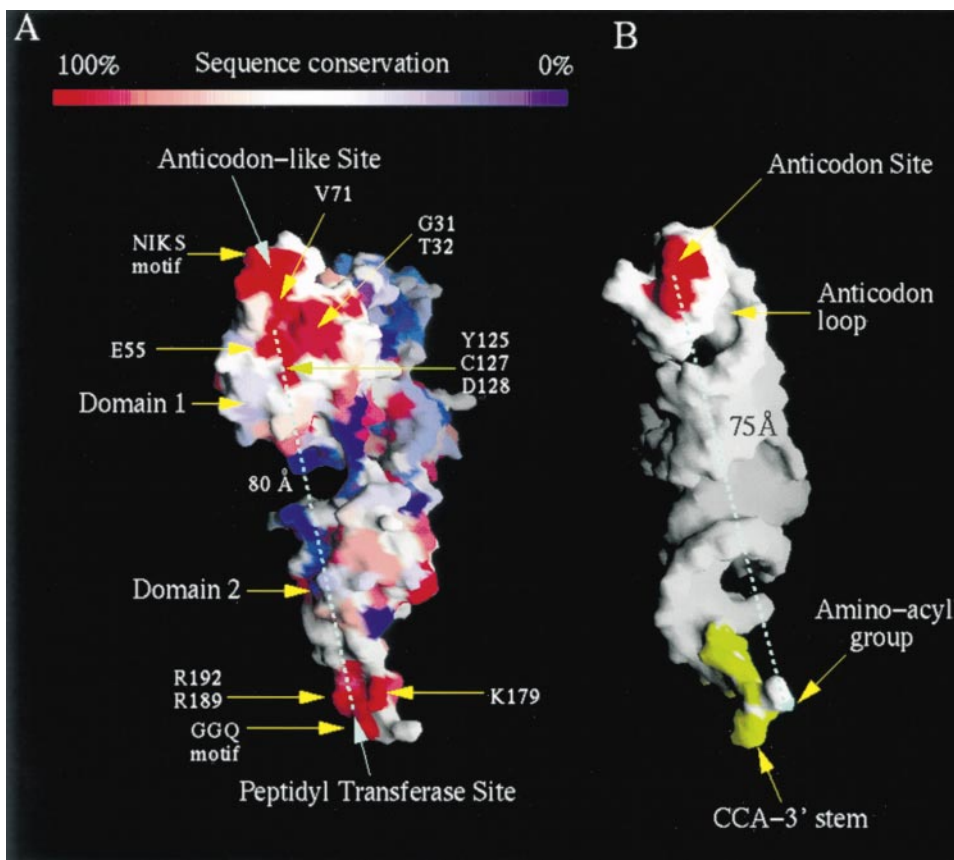


Figure 7. Molecular Surface Views of eRF1 and Yeast tRNA^{Phe}

(A) Molecular surface of eRF1 revealing regions of high to low sequence conservation between eukaryotic eRF1 and Archaea RF sequences, corresponding to a color ramp from red to blue, respectively. The figure depicts the conserved groove present on domain 1, and invariant residues including the NIKS motif (residues 62–65) are labeled. The molecule is rotated 90° relative to the view in Figures 1A and 4B.

(B) View of yeast tRNA^{Phe} showing the relative disposition of the anticodon bases and the amino group of an aminoacyl residue attached to the CCA stem. The distance between these sites matches the distance between the conserved groove on domain 1 of eRF1 and Gln-185 of the GGQ motif.

some similarities to a tRNA molecule, consistent with the functional similarities of release factors and tRNA, although these are not as envisaged by Ito et al. (1996). Our prediction that the family of prokaryotic and mitochondrial class 1 release factors differs in structure from their eukaryotic/Archaea counterpart suggests that these two families of release factors evolved independently from one another, implying that release factor activity mediated by proteins may have evolved subsequently to the divergence of the prokaryotes from the eukaryotes and Archaea. The occurrence of a universal GGQ motif in all release factors may reflect the highly conserved structure of the peptidyl transferase center in all ribosomes or, as proposed by Frolova et al. (1999), the requirement to interact with the invariant CCA stem of the P site peptidyl-tRNA molecule.

Experimental Procedures

Cloning and Protein Purification

Human eRF1 was overproduced using a bacterial expression system (Andjelkovic et al., 1996). The protein was purified using Ni-NTA agarose chromatography, anion exchange with a Mono Q column

(Pharmacia), and gel filtration using a Superdex 75 column (Pharmacia). The eluted protein was concentrated to ~10 mg/ml for crystallizations.

Crystallization and Heavy Atom Derivatives

Crystals of human eRF1 were grown at 20°C by hanging drop vapor diffusion. Equal volumes of protein solution were mixed with the precipitant solution (100 mM HEPES [pH 7.5], 14%–22% (w/v) PEG 4000, 15% (v/v) glycerol, and 200 mM NaCl). The crystals reached typical dimensions of 0.5 mm × 0.4 mm × 0.4 mm over a period within 1 week. Heavy-atom derivatives were prepared by soaking the crystals in stabilizing solutions containing 2 mM HgCl₂ (18 hr), 20 mM tri-methyl lead acetate (TMLA, 2 weeks), and 2 mM HgCl₂ + 20 mM TMLA (12 hr), respectively, before data collection.

Data Collection and Structure Determination

Structure determination was achieved using a combination of MIRAS and MAD methods. Crystals were transferred to the stabilizing solution including 25% (v/v) glycerol and fast frozen in a nitrogen gas stream at 100 K. Data were processed with MOSFLM and CCP4 (CCP4, 1994). The crystals belong to the space group P4₃2₁2, with the cell parameters a = b = 77.08 Å, c = 194.44 Å with a solvent content of 56%.

Heavy-atom parameters were refined and phases calculated with MLPHARE (Otwinowski, 1991; CCP4, 1994). The initial electron density map was improved by solvent flattening using the program DM

(CCP4, 1994; Cowtan and Main, 1996). The resultant electron density map was of insufficient quality for model building, as a consequence of the nonisomorphism between native and derivative eRF1 crystals. Data collection and phasing statistics using the MIRAS approach are summarized in Table 1.

Se-Met MAD data were collected at four different wavelengths (λ_1 : peak, λ_2 : inflection point; λ_3 : remote, λ_4 : 2nd inflection point) at station BW7A, EMBL (Hamburg, Germany). All diffraction data were recorded on a MAR image plate and processed with MOSFLM and CCP4 (CCP4, 1994) program packages. Seven out of the eight Se atoms per crystallographic asymmetric unit were located from the Bijvoet difference Fourier map using the data at the peak wavelength with phases derived from the MIRAS procedure described above. Heavy-atom parameter refinement and phase calculations were performed with the program SHARP (De la Fortelle and Bricogne, 1997) by treating the data as a special case of multiple isomorphous replacement (Ramakrishnan et al., 1993). The improved MAD phases from SOLOMON (Abrahams and Leslie, 1996) were combined with the MIRAS phases from DM using SIGMAA (Read, 1986). The electron density map calculated using the combined phases was of sufficient quality to allow tracing of the polypeptide chain.

Model Building and Refinement

The model was built using the program O (Jones et al., 1991) and refined with CNS (Brunger et al., 1998) using all data between 20.0 and 2.8 Å resolution. The phases calculated with the refined model were combined with the experimental phases (MIRAS and MAD) and improved further by solvent flattening using the program DM (CCP4, 1994; Cowtan and Main, 1996), allowing more residues to be built based on the improved electron density map. The Ramachandran plot shows that 92% of residues are either in the most favorable or additional allowed region with only 2.8% residues in the disallowed region. The refinement statistics are summarized in Table 1.

Effects of SUP45 [*sup45*] Mutations in Yeast

The shuffling strain Δ LE2[pUKC803] used is a haploid strain, with a chromosomal disruption of the essential *SUP45* gene (Stansfield et al., 1996) that is complemented by the single-copy *URA3-SUP45*⁺ plasmid pUKC803. Plasmid pUKC1901 was generated by cloning a Sall-XhoI fragment from pUKC803, carrying the *SUP45* gene with its native promoter, into similarly digested pRS315 (Sikorski and Hieter, 1989) to make a *LEU2* single copy plasmid carrying the *SUP45* gene. pUKC1901 derivatives were obtained by site-directed mutagenesis using the QuickChange mutagenesis kit (Stratagene). Transformation of Δ LE2[pUKC803] with pUKC1901 or its derivatives was performed as described previously (Gietz and Woods, 1994). Yeast strains were grown on YEPD or Minimal Medium supplemented with the suitable amino acids as described (Stansfield et al., 1996). To select yeast transformants that had lost the *URA3* plasmid pUKC803, FOA was added to the medium at a final concentration of 1g/l. Strain Δ LE2 carries the weak ochre suppressor tRNA *SUQ5* and the *ade2-1* ochre mutation, the latter of which confers adenine auxotrophy and a red phenotype on YEPD medium. A termination defect due to a mutation in *SUP45* would allow *SUQ5*-mediated translation of the *ade2-1* allele leading to adenine prototrophy and a white phenotype on YEPD medium.

Acknowledgments

We thank staff at the Synchrotron Radiation Source, Daresbury, and Dr. E. Pohl at BW7A (EMBL, Hamburg) for assistance and access to synchrotron radiation facilities. The work was supported by grants from the European Union Framework IV Programme and Human Frontiers Science Program to D. B. and B. A. H. and the Biotechnology and Biological Science Research Council to D. B. and M. F. T. We are very grateful to Drs. I. Stansfield and G. Bertram for communicating their results prior to publication and thank Dr. N. Andjelkovic for her contributions to the early stages of this project.

Received November 10, 1999; revised January 5, 2000.

References

- Abrahams, J.P., and Leslie, A.G.W. (1996). Methods used in the structure determination of the bovine mitochondrial F1 ATPase. *Acta Crystallogr. D* 52, 30–42.
- Åvarsson, A., Brazhnikov, E., Garber, M., Zheltonosova, J., Chirgadze, Y., al-Karadagh, S., Svensson, L.A., and Liljas, A. (1994). Three-dimensional structure of the ribosomal translocase: elongation factor G from *Thermus thermophilus*. *EMBO J.* 13, 3669–3677.
- Andjelkovic, N., Zolnierowicz, S., Van Hoof, C., Goris, J., and Hemmings, B.A. (1996). The catalytic subunit of protein phosphatase 2A associates with the translation termination factor eRF1. *EMBO J.* 15, 7156–7167.
- Barton, G.J. (1990). Protein multiple sequence alignment and flexible pattern matching. *Methods Enzymol.* 183, 403–428.
- Barton, G.J. (1993). ALSCRIPT: a tool to format multiple sequence alignments. *Protein Eng.* 6, 37–40.
- Bonetti, B., Fu, L., Moon, J., and Bedwell, D.M. (1995). The efficiency of translation termination is determined by a synergistic interplay between upstream and downstream sequences in *Saccharomyces cerevisiae*. *J. Mol. Biol.* 251, 334–345.
- Brown, C.M., and Tate, W.P. (1994). Direct recognition of mRNA stop signals by *Escherichia coli* polypeptide chain release factor 2. *J. Biol. Chem.* 269, 33164–33170.
- Brown, C.M., Stockwell, P.A., Trotman, C.N., and Tate, W.P. (1990). The signal for the termination of protein synthesis in prokaryotes. *Nucleic Acids Res.* 18, 2079–2086.
- Brünger, A.T., Adams, P.D., Clore, G.M., Delane, W.L., Gros, P., Grosse-Kunstleve, R.W., Jiang, J.S., Kuszewski, J., Nilges, M., Pannu, N.S., et al. (1998). Crystallography and NMR system: a new software suite for macromolecular structure determination. *Acta Crystallogr. D* 54, 905–921.
- Buckingham, R.H., Grentzmann, G., and Kisselev, L. (1997). Polypeptide chain release factors. *Mol. Microbiol.* 24, 449–456.
- Cate, J.H., Yusupov, M.M., Yusupova, G.Z., Earnest, T.N., and Noller, H.F. (1999). X-ray crystal structures of 70S ribosome functional complexes. *Science* 285, 2095–2104.
- CCP4 (Collaborative Computational Project no. 4.) (1994). The CCP4 Suite: programs for protein crystallography. *Acta Crystallogr. D* 50, 760–763.
- Cowtan, K., and Main, P. (1996). Phase combination and cross validation in iterated density-modification calculations. *Acta Crystallogr. D* 52, 43–48.
- Czworkowski, J., Wang, J., Steitz, T.A., and Moore, P.B. (1994). The crystal structure of elongation factor G complexed with GDP, at 2.7 Å resolution. *EMBO J.* 13, 3661–3668.
- De la Fortelle, E., and Bricogne, G. (1997). Maximum-likelihood heavy-atom parameters refinement in the MIR and MAD methods. *Methods Enzymol.* 276, 472–494.
- Eggertsson, G., and Soll, P. (1988). Transfer RNA-mediated suppression of termination codons in *E. coli*. *Microbiol. Rev.* 52, 354–379.
- Eurwilaichitr, L., Graves, F.M., Stansfield, I., and Tuite, M.F. (1999). The C-terminus of eRF1 defines a functionally important domain for translation termination in *Saccharomyces cerevisiae*. *Mol. Microbiol.* 32, 485–496.
- Freistoffer, D.V., Pavlov, M.Y., MacDougall, J., Buckingham, R.H., and Ehrenberg, M. (1997). Release factor RF3 in *E. coli* accelerates the dissociation of release factors RF1 and RF2 from the ribosome in a GTP-dependent manner. *EMBO J.* 16, 4126–4133.
- Frolova, L., Le Goff, X., Rasmussen, H.H., Cheperegin, S., Drugeon, G., Kress, M., Arman, I., Haenni, A.L., Celis, J.E., Philippe, M., et al. (1994). A highly conserved eukaryotic protein family possessing properties of polypeptide chain release factor. *Nature* 372, 701–703.
- Frolova, L., Goff, X.L., Zhouravleva, G., Davydova, E., Philippe, M., and Kisselev, L. (1996). Eukaryotic polypeptide chain release factor eRF3 is an eRF1- and ribosome dependent guanosine triphosphatase. *RNA* 2, 334–341.
- Frolova, L.Y., Tsivkovskii, R.Y., Sivolobova, G.F., Oparina, N.Y., Serpinsky, O.I., Blinov, V.M., Tatkov, S.I., and Kisselev, L.L. (1999). Mutations in the highly conserved GGQ motif of class 1 polypeptide

- release factors abolish ability of human eRF1 to trigger peptidyl-tRNA hydrolysis. *RNA* 5, 1014–1020.
- Gietz, R.D., and Woods, R.A. (1994). In *Molecular Genetics of Yeast: A Practical Approach*, J.R. Johnston, ed. (Oxford: IRL Press), pp. 121–134.
- Goldstein, J.L., Beaudet, A.L., and Caskey, C.T. (1970). Peptide chain termination with mammalian release factor. *Proc. Natl. Acad. Sci. USA* 67, 99–106.
- Grentzmann, G., and Kelly, P.J. (1997). Ribosomal binding site of release factors RF1 and RF2. A new translational termination assay in vitro. *J. Biol. Chem.* 272, 12300–12304.
- Grentzmann, G., Brechemier-Baey, D., Heurgue, V., Mora, L., and Buckingham, R.H. (1994). Localization and characterization of the gene encoding release factor RF3 in *Escherichia coli*. *Proc. Natl. Acad. Sci. USA* 91, 5848–5852.
- Ito, K., Ebihara, K., Uno, M., and Nakamura, Y. (1996). Conserved motifs in prokaryotic and eukaryotic polypeptide release factors: tRNA-protein mimicry hypothesis. *Proc. Natl. Acad. Sci. USA* 93, 5443–5448.
- Ito, K., Ebihara, K., and Nakamura, Y. (1998). The stretch of C-terminal acidic amino acids of translational release factor eRF1 is a primary binding site for eRF3 of fission yeast. *RNA* 4, 958–972.
- Jones, T.A., Zou, J.Y., Cowan, S.W., and Kjeldgaard, M. (1991). Improved methods for building protein models in electron density maps and the location of errors in these models. *Acta Crystallogr. A* 47, 489–501.
- Konecki, D.S., Aune, K.C., Tate, W., and Caskey, C.T. (1977). Characterization of reticulocyte release factor. *J. Biol. Chem.* 252, 4514–4520.
- Kraulis, P.J. (1991). MOLSCRIPT: a program to produce both detailed and schematic plots of protein structures. *J. App. Crystallog.* 24, 946–950.
- McCaughan, K.K., Poole, E.S., Pel, H.J., Mansell, J.B., Mannering, S.A., and Tate, W.P. (1998). Efficient in vitro translation termination in *E. coli* is constrained by the orientations of the release factor, stop signal and peptidyl-tRNA within the termination complex. *Biol. Chem.* 379, 857–866.
- Merit, E.A., and Murphy, M.E.P. (1994). Raster3D Version 2.0. A program for photorealistic molecular graphics. *Acta Crystallogr. D* 50, 869–873.
- Merkulova, T.I., Frolova, L.Y., Lazar, M., Camonis, J., and Kisselev, L.L. (1999). C-terminal domains of human translation termination factors eRF1 and eRF3 mediate their in vivo interaction. *FEBS Lett.* 443, 41–47.
- Mikuni, O., Ito, K., Moffat, J., Matsumura, K., McCaughan, K., Nobukuni, T., Tate, W., and Nakamura, Y. (1994). Identification of the prfC gene, which encodes peptide-chain-release factor 3 of *Escherichia coli*. *Proc. Natl. Acad. Sci. USA* 91, 5798–5802.
- Millman, G., Goldstein, J., Scolnick, E., and Caskey, T. (1969). Peptide chain termination. 3. Stimulation of in vitro termination. *Proc. Natl. Acad. Sci. USA* 63, 183–190.
- Mironova, L.N., Zelenaya, O.A., and Ter-Avanesyan, M.D. (1986). Nuclear-mitochondrial-interactions in yeast: mitochondrial mutations compensating respiratory deficiency of sup1 and sup2 mutants. *Genetica (Russia)* 22, 200–208.
- Moffat, J.G., and Tate, W.P. (1994). A single proteolytic cleavage in release factor 2 stabilizes ribosome binding and abolishes peptidyl-tRNA hydrolysis activity. *J. Biol. Chem.* 269, 18899–18903.
- Mottagui-Tabar, S., Tuite, M.F., and Isaksson, L.A. (1998). The influence of the 5' codon context on translation termination in *Saccharomyces cerevisiae*. *Eur. J. Biochem.* 257, 249–254.
- Nagai, K., Oubridge, C., Ito, N., Avis, J., and Evans, P. (1995). The RNP domain: a sequence-specific RNA-binding domain involved in processing and transport of RNA. *Trends Biochem. Sci.* 20, 235–240.
- Nakamura, Y., and Ito, K. (1998). How protein reads the stop codon and terminates translation. *Genes Cells* 3, 265–278.
- Nicholls, A., Sharp, K., and Honig, B. (1991). Protein folding and association: insights from the interfacial and thermodynamic properties of hydrocarbons. *Proteins* 11, 281–296.
- Nissen, P., Kjeldgaard, M., Thirup, S., Polekhina, G., Reshetnikova, L., Clark, B.F., and Nyborg, J. (1995). Crystal structure of the ternary complex of Phe-tRNA^{Phe}, EF-Tu, and a GTP analog. *Science* 270, 1464–1472.
- Noller, H.F., Hoffarth, V., and Zimniak, L. (1992). Unusual resistance of peptidyl-transferase to protein extraction procedures. *Science* 256, 1416–1419.
- Pannifer, A.D., Flint, A.J., Tonks, N.K., and Barford, D. (1998). Visualisation of the cysteinyl-phosphate intermediate of a protein tyrosine phosphatase by X-ray crystallography. *J. Biol. Chem.* 273, 10454–10462.
- Otwinowski, Z. (1991). Maximum likelihood refinement of heavy-atom parameters. In *Isomorphous Replacement and Anomalous Scattering*. Proceedings of the CCP4 Study Weekend, 25–26, W. Wolf, P.R. Evans, and A.G.W. Leslie, eds. (Warrington, UK: SERC Daresbury Laboratory), pp. 80–86.
- Poole, E.S., Brown, C.M., and Tate, W.P. (1995). The identity of the base following the stop codon determines the efficiency of in vivo translational termination in *Escherichia coli*. *EMBO J.* 14, 151–158.
- Poole, E.S., Brimacombe, R., and Tate, W.P. (1997). Decoding the translational termination signal: the polypeptide chain release factor in *Escherichia coli* crosslinks to the base following the stop codon. *RNA* 3, 974–982.
- Ramakrishnan, V., Finch, C.T., Graziano, V., Lee, P.J., and Sweet, R.M. (1993). Crystal structure of globular domain of histone H5 and its implications for nucleosome binding. *Nature* 362, 219–223.
- Read, R.J. (1986). Improved Fourier Coefficients for maps using phases from partial structures with errors. *Acta Crystallogr. A* 42, 140–149.
- Scheffzek, K., Ahmadian, M.R., Kabsch, W., Wiesmuller, L., Lautwein, A., Schmitz, F., and Wittinghofer, A. (1997). The Ras-RasGAP complex: structural basis for GTPase activation and its loss in oncogenic Ras mutants. *Science* 227, 333–338.
- Scolnick, E., Tompkins, R., Caskey, T., and Nirenberg, M. (1968). Release factors differing in specificity for terminator codons. *Proc. Natl. Acad. Sci. USA* 61, 768–774.
- Sikorski, R.S., and Hieter, P. (1989). A system of shuttle vectors and yeast host strains designed for efficient manipulation of DNA in *Saccharomyces cerevisiae*. *Genetics* 122, 19–27.
- Stansfield, I., Jones, K.M., Kushnirov, V.V., Dagkesamanskaya, A.R., Poznyakovski, A.I., Paushkin, S.V., Nierras, C.R., Cox, B.S., Ter-Avanesyan, M.D., and Tuite, M.F. (1995a). The products of the SUP45 (eRF1) and SUP35 genes interact to mediate translation termination in *Saccharomyces cerevisiae*. *EMBO J.* 14, 4365–4373.
- Stansfield, I., Akhmaloka, and Tuite, M.F. (1995b). A mutant allele of the SUP45 (SAL4) gene of *Saccharomyces cerevisiae* shows temperature-dependent allosuppressor and omnipotent suppressor phenotypes. *Curr. Genet.* 27, 417–426.
- Stansfield, I., Eurwilaichitr, L., Akhmaloka, and Tuite, M.F. (1996). Depletion in the levels of the release factor eRF1 causes a reduction in the efficiency of translation termination in yeast. *Mol. Microbiol.* 20, 1135–1143.
- Stansfield, I., Kushnirov, V.V., Jones, K.M., and Tuite, M.F. (1997). A conditional-lethal translation termination defect in a sup45 mutant of the yeast *Saccharomyces cerevisiae*. *Eur. J. Biochem.* 245, 557–563.
- Tate, W., Greuer, B., and Brimacombe, R. (1990). Codon recognition in polypeptide chain termination: site directed crosslinking of termination codons to *Escherichia coli* release factor 2. *Nucleic Acids Res.* 18, 6537–6544.
- Zhouravleva, G., Frolova, L., Le Goff, X., Le Guellec, R., Inge-Vechtomov, S., Kisselev, L., and Philippe, M. (1995). Termination of translation in eukaryotes is governed by two interacting polypeptide chain release factors, eRF1 and eRF3. *EMBO J.* 14, 4065–4072.

Protein Data Bank ID Code

Coordinates have been deposited with ID code 1DT9.